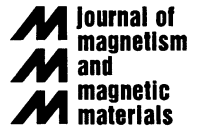




ELSEVIER

Journal of Magnetism and Magnetic Materials 220 (2000) 161–166



www.elsevier.com/locate/jmmm

Transport and magnetic properties of $\text{La}_{0.8}\text{Ce}_{0.2}\text{MnO}_3$ thin films grown by pulsed laser deposition

Y.G. Zhao*, R.C. Srivastava, P. Fournier, V. Smolyaninova, M. Rajeswari, T. Wu, Z.Y. Li, R.L. Greene, T. Venkatesan

Center for Superconductivity Research, Department of Physics, University of Maryland, College Park, MD 20742, USA

Received 13 June 2000

Abstract

We report on the growth of $\text{La}_{0.8}\text{Ce}_{0.2}\text{MnO}_3$ thin films on (001) LaAlO_3 substrates by pulsed laser deposition. CeO_2 as an impurity is present in both the bulk and film samples. The electrical transport and magnetic properties of the films are similar to that of the divalent cation-doped or La deficient LaMnO_3 , which show colossal magnetoresistance. Thermopower measurements indicate that the carriers are holes. The results are explained in terms of a La site deficiency due to the existence of CeO_2 . © 2000 Elsevier Science B.V. All rights reserved.

PACS: 81.15.Fg; 75.70. – I; 73.50. – h

Keywords: Thin films; Transport properties; Magnetic properties

The discovery of the colossal magnetoresistance (CMR) in $\text{R}_{1-x}\text{A}_x\text{MnO}_3$ (R = rare earth elements, A = divalent cations) has renewed the interest in the manganese oxides because of their importance for both fundamental issues in condensed matter physics and possible applications [1–3]. The undoped parent compound LaMnO_3 (LMO) is an antiferromagnetic insulator and Mn^{3+} is a Jahn–Teller ion with the electronic configuration $t_{2g}^3e_g^1$ and the occupied e_g band is the Jahn–Teller split lower e_g band. When doped on the La sites with divalent cations, such as Ca^{2+} , Sr^{2+} , Ba^{2+} , etc., holes are introduced into the Jahn–Teller split

lower e_g band and Mn ions show mixed valence of $\text{Mn}^{3+}/\text{Mn}^{4+}$. Within certain doping range, the material shows insulator–metal transition and paramagnetic–ferromagnetic transition at certain temperature (T_p). In the presence of a magnetic field, transport between adjacent FM regions is enhanced (CMR effect) owing to spin alignment and a concomitant double exchange mechanism [4–6]. In order to quantitatively define the CMR materials, it was found that Jahn–Teller effect also plays an important role [7,8] besides the double exchange mechanism. The effect of divalent cation doping has been widely investigated. However, in analogy to the electron-doped superconductor $\text{Nd}_{2-x}\text{Ce}_x\text{CuO}_4$ in high- T_c superconductors, there are a few reports [9–11] about using possible tetravalent Ce^{4+} , instead of divalent cations, to dope on the La sites in order to obtain electron-doped bulk CMR materials with Mn mixed valence

*Corresponding author. Present address: Department of Physics, Tsinghua University, Beijing 100084, People's Republic of China. Tel.: +86-10-62772764; fax: +86-10-62781604.

E-mail address: ygzha@tsinghua.edu.cn (Y.G. Zhao).

of $\text{Mn}^{2+}/\text{Mn}^{3+}$. In this scenario, the doped electrons occupy the Jahn–Teller split upper e_g band. However, some issues are not clear yet. For example, is the Ce-doped LMO in a single phase or do all the doped Ce go into the La site? The issue related to Ce-doped LMO is important and deserves further study.

In this paper, we report on the growth of $\text{La}_{0.8}\text{Ce}_{0.2}\text{MnO}_3$ thin films on LaAlO_3 substrates by pulsed laser deposition (PLD). We also studied the electrical transport and magnetic properties of the films. Our results show that a CeO_2 impurity phase always exists in both Ce-doped LMO bulk and thin films, and the presence of CeO_2 introduces vacancies on the La sites. The observed CMR effect can be explained in terms of the doping of holes due to these vacancies.

$\text{La}_{0.8}\text{Ce}_{0.2}\text{MnO}_3$ thin films were grown on (001) LaAlO_3 substrates by PLD using high quality $\text{La}_{0.8}\text{Ce}_{0.2}\text{MnO}_3$ target from Micro Ceramics Inc. The laser energy was $2\text{J}/\text{cm}^2$ at a wavelength of 248 nm and the laser pulse repetition frequency was 8 Hz. Several substrate temperatures and deposition pressures were used in order to get single phase films. It was found that the films deposited at substrate temperature of 800°C in 300 mTorr of oxygen with a cool down in 400 Torr of oxygen have less amount of impurity phase. The thickness of the films was about 150 nm. Rutherford back scattering (RBS) was used to measure the composition of the films. A Siemens D5000 diffractometer equipped with a Huber 4 circle Goniometer was used for X-ray studies and the Siemens P30 program was used for measuring reflections and calculating the lattice parameters. The resistivity was measured using a four-probe technique on patterned and unpatterned thin films with both DC and AC currents. For the thermopower measurements, a thin film is epoxied onto a copper mount (heat sink) on one side while a small thin-film heater is attached to the other side. A differential thermocouple (chromel-constantan), with its two tips attached onto the sample with GE varnish, measures the applied temperature gradient ($\nabla_x T$) $\leq 0.2\text{K}/\text{mm}$. The thermoelectric voltage is measured with pre-calibrated gold wires attached onto the film. Both voltages from the sample and the differential thermocouple are measured simul-

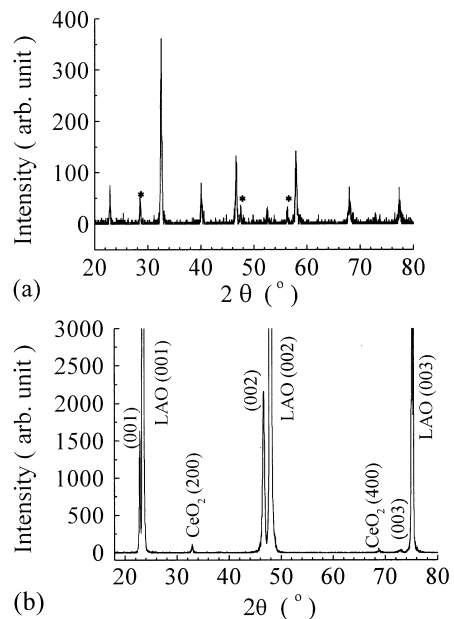


Fig. 1. X-ray diffraction patterns for (a) $\text{La}_{0.8}\text{Ce}_{0.2}\text{MnO}_3$ target, the stars indicate the peaks from CeO_2 impurity, and (b) $\text{La}_{0.8}\text{Ce}_{0.2}\text{MnO}_3$ thin films.

taneously while the temperature gradient is ramped up slowly. From the linear relation between the two voltages, we can extract the slope giving $S = E_x/\nabla_x T$, adding a statistical estimate (uncertainty) on the absolute value. The typical uncertainty obtained with such a method is of the order of $\pm 0.1\ \mu\text{V}/\text{K}$. For the measurement of magnetic property of the samples, a SQUID magnetometer was used.

Fig. 1(a) shows the XRD patterns for $\text{La}_{0.8}\text{Ce}_{0.2}\text{MnO}_3$ target. There are three peaks (marked with stars) at 28.47° , 47.47° and 56.33° , respectively. These peaks were not present in the XRD patterns of the divalent doped or La deficient LMO samples. Analysis shows that these peaks can be well fitted both in angles and intensities by the three strongest peaks of CeO_2 with index ¹ (1 1 1), (2 2 0) and (3 1 1). These peaks were also present in the XRD patterns of the Ce-doped LMO bulk samples, however, Mandal and Das [9,10] assigned

¹JCPDS Powder Diffraction File34-394

these peaks to the Ce-doped LMO phase and thus concluded that their Ce-doped LMO bulk is single phase. Gebhardt et al. also prepared Ce-doped LMO bulk samples [11]. They found that an impurity phase was present and the amount of the impurity phase increases with the doping level. They did not show the XRD patterns of their samples and believed that the impurity was MnO_2 based on the magnetic measurement. However, MnO_2 does not fit the three peaks in the XRD patterns though some traces of MnO_2 may be present. In fact, we also prepared some Ce-doped bulk samples and the XRD pattern of the samples similar to that reported by Mandal and Das [10], and to that of the target. Fig. 1(b) shows the XRD pattern of $\text{La}_{0.8}\text{Ce}_{0.2}\text{MnO}_3$ films and the pattern is similar to that of the divalent cation-doped LMO films, except for the two peaks at 32.8 and 68.9° . In fact, these two peaks are also present in the divalent cation-doped LMO films when the film growth conditions are not optimized and are assigned to the (1 1 0) and (2 2 0) reflections of the divalent cation-doped LMO phase. It is tempting to think that the same assignment may also apply to the $\text{La}_{0.8}\text{Ce}_{0.2}\text{MnO}_3$ thin films. However, careful measurements on the films showed that these two peaks correspond to (2 0 0) and (4 0 0) reflections of CeO_2 .

Eighteen reflections of (0 0 l), (h 0 l), (0 k l) and (h k l) families which had adequate intensity for measurement were centered in χ , ϕ , ω and 2θ using the Siemens P30 program. Least squares calculation on these reflections gave the lattice parameters of the main phase $\text{La}_{0.8}\text{Ce}_{0.2-x}\text{MnO}_3$ as $a = 0.3852$ nm, $b = 0.3857$ nm, $c = 0.3903$ nm in an orthorhombic unit cell. If we assume simultaneous presence of [1 1 0] and [0 0 1] orientations in the films and assign the two peaks at 32.8 and 68.9° to (1 1 0) and (2 2 0) reflections of the films, as in the divalent cation-doped LMO case, it will require a and b to be at about 45° in χ . Reflections corresponding to (2 0 0) and (0 2 0) were located but these gave a and b equal to 0.3828 and 0.3830 nm, respectively, which are considerably different from those determined from [0 0 1] orientation of the same film. Moreover, reflections of (1 0 1), (0 1 1), (0 1 1) and (1 0 1), which would occur at a 2θ and χ of about 32.5 and 60° , respectively, and are quite in-

tense (only next to (0 0 2) in intensity) could not be found. The assumption of [1 0 1] instead of [1 1 0] for the orientation results in similar anomaly. The origin of these two peaks was, therefore, sought in the presence of some impurity. These peaks match with the (2 0 0) and (4 0 0) reflections from CeO_2 , (see footnote 1) which is the most likely impurity, as it is also present in the bulk. CeO_2 has grown epitaxially in the films such that its a and b -axis match with d_{110} and $d_{\bar{1}\bar{1}0}$ of the LAO substrate. With this assignment of the extra peaks, 14 more CeO_2 reflections of (0 0 l), (h 0 l), (0 k l) and (h k l) families with adequate intensity were located for measurement. These reflections were centered in χ , ϕ , ω and 2θ using the Siemens P30 program and the lattice parameters determined by least squares calculation are $a = 0.5399(8)$ nm, $b = 0.5407(9)$ nm, $c = 0.5430(5)$ nm in an orthorhombic unit cell. Within experimental error, a equals to b . It may be pointed out that CeO_2 has cubic structure in bulk samples (see footnote 1) with $a = 0.54113(1)$ nm. We found a slight elongation in c , which is the out of plane direction in the film. This elongation may be due to the compressive strain in the plane arising from lattice mismatch between CeO_2 and LAO ($d_{110} = 0.5359$ nm) substrate. It is, therefore, concluded that Ce-doped LMO samples contain both CeO_2 and $\text{La}_{0.8}\text{Ce}_{0.2-x}\text{MnO}_3$ phases.

Fig. 2 shows the temperature dependence of the resistance for the target. The resistance of the target increases with decreasing temperature and shows a peak around 210 K and then decreases with an

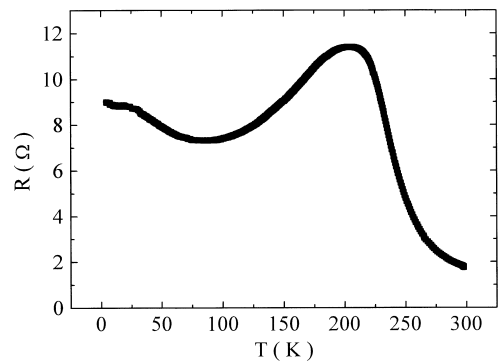


Fig. 2. Temperature dependence of the resistance for $\text{La}_{0.8}\text{Ce}_{0.2}\text{MnO}_3$ target.

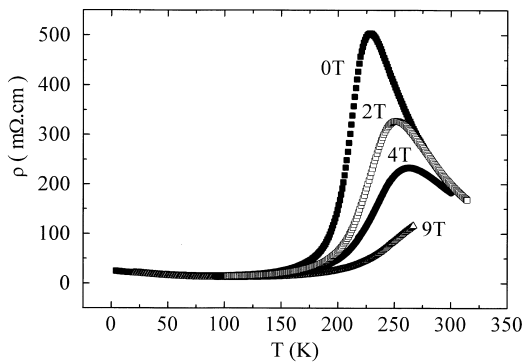


Fig. 3. Temperature dependence of the resistance for $\text{La}_{0.8}\text{Ce}_{0.2}\text{MnO}_3$ films under different magnetic fields.

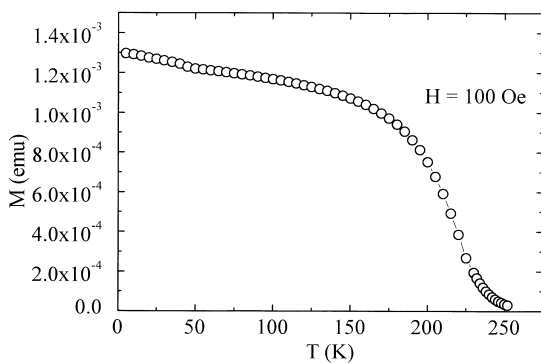


Fig. 4. Temperature dependence of the magnetization for $\text{La}_{0.8}\text{Ce}_{0.2}\text{MnO}_3$ films.

upturn at lower temperatures. This behavior is similar to that reported by Das and Mandal for Ce-doped LMO bulk samples [9,10]. Fig. 3 shows the temperature dependence of the resistivity under different magnetic fields for films with nominal composition of $\text{La}_{0.8}\text{Ce}_{0.2}\text{MnO}_3$. It shows that the behavior is similar to that of the CMR materials. Fig. 4 shows the temperature dependence of the magnetization for the films and it shows a ferromagnetic transition around 210 K, consistent with the insulator–metal transition temperature in Fig. 3.

In Fig. 5, we show overlapped plots of the temperature dependence of the thermopower and the resistivity for $\text{La}_{0.8}\text{Ce}_{0.2}\text{MnO}_3$ films indicating the correspondence of the transition as measured on

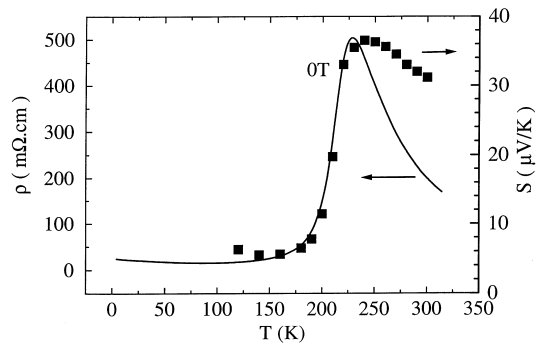


Fig. 5. Temperature dependence of the thermopower and resistivity for $\text{La}_{0.8}\text{Ce}_{0.2}\text{MnO}_3$ films.

the same sample by two different transport properties. Using $\rho = \rho_0 T^n \exp(E_a/k_B T)$ for the temperature dependence of the resistivity [with $n = 0, 1$ (adiabatic polaron) and 1.5 (non-adiabatic polaron)] [12,13], we can extract the carrier activation energy for the non-metallic resistivity above peak temperature. Despite a narrow range of temperature to fit the data, we obtain $E_a = 92, 116$ and 128 meV for $n = 0, n = 1$ and $n = 1.5$, respectively. Jaime et al. studied the electrical transport property of $\text{La}_{2/3}\text{Ca}_{1/3}\text{MnO}_3$ films [14] and they found an activation energy in the adiabatic limit to be 112 meV, which is very close to the 116 meV obtained in our experiment for the Ce-doped LMO films. For $\text{La}_{0.7}\text{Ce}_{0.3}\text{MnO}_3$ bulk samples, the activation energy is 165 meV as reported by Mandal and Das [10]. As shown in Fig. 5, the thermopower is positive and can be explained by hole doping rather than electron doping. Mandal and Das [10] reported that the thermopower of the as-prepared $\text{La}_{0.7}\text{Ce}_{0.3}\text{MnO}_3$ bulk samples became negative below 100 K, while the thermopower of the annealed bulk samples was always positive. Because the resistivity of the as-prepared bulk samples is very high, it may be difficult to get reliable thermopower results. Even though the temperature dependence of the resistivity for the as-prepared $\text{La}_{0.7}\text{Ce}_{0.3}\text{MnO}_3$ and $\text{Pr}_{0.7}\text{Ce}_{0.3}\text{MnO}_3$ are quite different, [10] it should be also pointed out that they show a change in the sign of thermal power at the same temperature, which is surprising. Fitting the limited data of thermoelectric power above the

peak temperature to $S(T) = (k_B/e)[\alpha + E_s/k_B T]$, where E_s is the activation energy for the thermopower and α is a sample dependent constant, we extract an activation energy close to 9 meV, which is one order of magnitude smaller than that deduced from the resistivity curves. Similar results were obtained for $\text{La}_{2/3}\text{Ca}_{1/3}\text{MnO}_3$ films by Jaime et al. [14]. The activation energy deduced from thermopower measurement was 10 meV and the difference of the activation energies deduced from resistivity and thermopower was claimed to be a characteristic of Holstein polarons [14].

The electrical transport and magnetic properties of the films with the nominal composition of $\text{La}_{0.8}\text{Ce}_{0.2}\text{MnO}_3$ can be understood if we consider the existence of CeO_2 in the films. The presence of CeO_2 introduces vacancies on the La sites and these vacancies cause self doping in the films. It has been shown that La deficiency in $\text{La}_{1-x}\text{MnO}_3$ can lead to similar CMR effect as divalent cation doping does [15–18] and x can even go to 0.33 as shown by Gupta et al. [15]. We also annealed the $\text{La}_{0.8}\text{Ce}_{0.2}\text{MnO}_3$ thin films at 850°C for 10 h and cooled down slowly, and the Curie temperature (T_c) increases to 260 K. This behavior is consistent with that of $\text{La}_{1-x}\text{MnO}_3$ and divalent cation-doped LMO. A T_c increase upon annealing in oxygen was also reported by Mandal and Das in their Ce-doped bulk samples [9,10]. It has been found that Ce may have some evaporation during the sintering of the target [19]. This evaporation will also introduce some vacancies on the La site and these La vacancies may be helpful for Ce to dope on La site during film growth. It has been shown that Ce is very difficult to be doped into $\text{Pr}_{1-x}\text{Ce}_x\text{Ba}_2\text{Cu}_3\text{O}_7$ and the melting temperature of the compound also decreases with the Ce doping [20]. Even for the electron-doped superconductor $\text{Nd}_{2-x}\text{Ce}_x\text{CuO}_4$, it seems that impurity phase containing Ce is always present [21]. Therefore, Ce doping may be different from other element doping. Recently, Raychaudhuri et al. also reported some work on the growth of $\text{La}_{0.7}\text{Ce}_{0.3}\text{MnO}_3$ films [22]. There are still CeO_2 peaks in the XRD pattern of the films, although small. Because of the Ce evaporation problem, it is difficult to say that the composition of the films is the same as the nominal composition. In fact, the T_c dependence

of their films with deposition pressure can also be explained by Ce evaporation dependence on the deposition pressure because more Ce is evaporated under low deposition pressure than that under high-deposition pressure. For $\text{La}_{0.7}\text{Ce}_{0.15}\text{Ca}_{0.15}\text{MnO}_3$, La site ion size disorder effect [23] and electron–phonon interaction should also be considered besides the carrier number. Therefore, it is important to determine the composition of the film to check whether it is consistent with the nominal composition. It is also essential to measure the valence of Ce ions and Mn ions in the films, and the type of carriers by Hall effect before one can definitely say something about electron–doped CMR.

In summary, we have grown $\text{La}_{0.8}\text{Ce}_{0.2}\text{MnO}_3$ films on LAO substrates. The films show CMR effect. A CeO_2 impurity phase was present in both bulk and films. The transport and magnetic results can be explained in terms of hole transport from self-doping effect due to the La site vacancies introduced by the CeO_2 impurity.

Acknowledgements

This work was supported by the NSF MRSEC under Grant No. DMR-9632521. YGZ would like to thank Liuwan Zhang at Tsinghua University for helpful discussion.

References

- [1] S. Chahara, T. Ohno, K. Kasai, Y. Kozono, Appl. Phys. Lett. 63 (1993) 1990.
- [2] R. von Helmolt, J. Wecker, B. Holzapfel, L. Schultz, K. Samwer, Phys. Rev. Lett. 71 (1993) 2331.
- [3] S. Jin, T.H. Tiefel, M. McCormack, R.A. Fastnacht, R. Ramesh, L.H. Chen, Science 264 (1994) 413.
- [4] C. Zener, Phys. Rev. 82 (1951) 403.
- [5] P.W. Anderson, H. Hasegawa, Phys. Rev. 100 (1955) 675.
- [6] P.G. de Gennes, Phys. Rev. 118 (1960) 141.
- [7] A.J. Millis, P.B. Littlewood, B.I. Shraiman, Phys. Rev. Lett. 74 (1995) 5144.
- [8] A.J. Millis, P.B. Littlewood, B.I. Shraiman, Phys. Rev. Lett. 77 (1996) 175.
- [9] S. Das, P. Mandal, Z. Phys. B 104 (1997) 7.
- [10] P. Mandal, S. Das, Phys. Rev. B 56 (1997) 15073.
- [11] J.R. Gebhardt, S. Roy, N. Ali, J. Appl. Phys. 85 (1999) 5390.

- [12] T. Holstein, *Ann. Phys.* 8 (1959) 343.
- [13] D. Emin, T. Holstein, *Ann. Phys.* 53 (1969) 439.
- [14] M. Jaime, M.B. Salamon, M. Rubinstein, R.E. Treece, J.S. Horwitz, D.B. Chrisey, *Phys. Rev. B* 54 (1996) 11914.
- [15] A. Gupta, T.R. McGuire, P.R. Duncombe, M. Rupp, J.Z. Sun, W.J. Gallagher, Gang Xiao, *Appl. Phys. Lett.* 67 (1995) 3494.
- [16] T.R. McGuire, A. Gupta, P.R. Duncombe, M. Rupp, J.Z. Sun, R.B. Laibowitz, W.J. Gallagher, *J. Appl. Phys.* 79 (1996) 4549.
- [17] S. Pignard, H. Vincent, J.P. Senateur, J. Pierre, A. Abrutis, *J. Appl. Phys.* 82 (1997) 4445.
- [18] Chun-Che Chen, Alexde Lozanne, *Appl. Phys. Lett.* 73 (1998) 3950.
- [19] S. Panda, private communication.
- [20] S.Y. Xiong, Y.G. Zhao, D.J. Dong, S.Q. Guo, P.C. Song, L.W. Zhang, M.H. Zhu, B.S. Cao, B.L. Gu, *Physica C* 282-287 (1997) 783.
- [21] D.P. Beesabathina, L. Salamanca-Riba, S.N. Mao, X.X. Xi, T. Venkatesan, *Appl. Phys. Lett.* 62 (1993) 3022.
- [22] P. Raychaudhuri, S. Mukherjee, A.K. Nigam, J. John, U.D. Vaisnav, R. Pinto, P. Mandal, *J. Appl. Phys.* 86 (1999) 5718.
- [23] L.M. Rodriguez-Martinez, J.P. Attfield, *Phys. Rev. B* 54 (1996) R15622.